LA-UR-79-808

TITLE: ENGINEERING DESIGN OF A DIRECT-CYLCE STEAM-GENERATING BLANKET FOR A LONG-PULSE FUSION REACTOR

AUTHOR(S): G. E. Cort, R. L. Hagenson, R. W. Teasdale, W. E. Fox, P. D. Soran, H. S. Cullingford, C. G. Bathke, and R. A. Krakowski

SUBMITTED TO: 5th International Conference on Structural Mechanics in Reactor Technology, Berlin, West Germany, August 13-17, 1979

NOTICE

This report was prepared as an account of work sponsored by the United States Government. Neither the United States nor the United States Department of Energy, nor any of their employees, nor any of their contractors, subcontractors, or their employees, makes any warranty, express or implied, or assumes any legal liability or responsibility for the accuracy, completeness or usefulness of any information, [illegible]

MASTER

By acceptance of this article, the publisher recognizes that the U.S. Government retains a nonexclusive, royalty-free license to publish or reproduce the published form of this contribution, or to allow others to do so, for U.S. Government purposes.

The Los Alamos Scientific Laboratory requests that the publisher identify this article as work performed under the auspices of the U.S. Department of Energy.

University of California

LOS ALAMOS SCIENTIFIC LABORATORY

Post Office Box 1663 Los Alamos, New Mexico 87545

An Affirmative Action/Equal Opportunity Employer

DISTRIBUTION OF THIS DOCUMENT IS UNLIMITED

ENGINEERING DESIGN OF A DIRECT-CYCLE STEAM-GENERATING BLANKET FOR A LONG-PULSE FUSION REACTOR

G. E. Cort, R. L. Hagenson, R. W. Teasdale, W. E. Fox, P. D. Soran,
H. S. Cullingford, C. G. Bathke, and R. A. Krakowski

Los Alamos Scientific Laboratory
Los Alamos, New Mexico 87545
USA

ABSTRACT

A comprehensive neutronics, thermohydraulic, and mechanical design of a tritium-breeding blanket for use by a conceptual long-pulse Reversed-Field Pinch Reactor (RFPR) is described. On the basis of constraints imposed by cost and the desire to use existing technology, a direct-cycle steam system and stainless-steel construction was used. For reasons of plasma stability, the RFPR blanket supports a 20-mm-thick copper first wall. Located behind the 1.5-m-radius first wall is a 0.50-m-thick stainless-steel blanket containing a granular bed of Li_2 through which flows low-pressure helium (0.1 MPa) for tritium extraction. Water/steam tubes radially penetrate this packed bed. The large thermal capacity and low thermal diffusivity of the Li_2O blanket are sufficient to maintain a nearly constant temperature during the ~ 25-s burn period (~ 80% duty factor). The copper first wall is cooled by circulating water (5.5 MPa, 310 K inlet, 460 K outlet), and approximately 38% of the total fusion power is removed by the separate first-wall coolant loop. Nuclear heating within the packed Li_2O bed is removed by water circulating in radial, close-spaced U-tubes (5.5 Pa, 422 K inlet, 551 K outlet). These steam-generating tubes are arrayed on 40-mm centers, use external fins to enhance and control heat transfer from the packed bed, and are manifolded at the outer diameter of each 2-m-long RFPR module. Exit steam conditions at 5.5 MPa correspond to 7.8 K superheat; bulk boiling typically occurs in the inlet leg at 0.2 m from the first wall, and dryout conditions occur 0.3 m from the first wall in the outlet leg. The steam cycle envisaged for the RFPR is similar to that used in a light-water nuclear power plant. This blanket design generates slightly superheated steam in a one-pass operation to eliminate the need for a secondary coolant loop and a separate steam generator. The thermohydraulic penalties associated with this more conventional mode of operation are quantified. Generally, the projected 26.5% cycle efficiency is limited by thermal mechanical constraints imposed by the 20-mm-thick copper first wall. Tritium is released from the Li_2O as T_2O and is swept from the blanket in the helium purge stream with negligible migration into the primary coolant loop. A low-temperature, organic-fluid, bottoming cycle uses part of the reject heat deposited into the separately cooled first wall. This blanket configuration has a tritium breeding ratio in excess of 1 1 and recovers >99% of a fusion energy; a remainder of the fusion energy is deposited in a 1.5-m-thick, room-temperature borated-water/steel magnet shields. The high aspect ratio (>10) RFPR affords considerable engineering simplification resulting from the highly modular blanket constructio

1. Introduction

The Reversed-Field Pinch [1] (RFP) is a high-beta toroidal device of arbitrary aspect ratio with a plasma current density that is sufficient to achieve ignition by ohmic heating alone. Confinement is provided primarily by the poloidal field with the concomitant economy of magnetic field and ease of magnet design. A conducting shell or external conductors would eliminate MHD modes with wavelengths in excess of the minor radius. External conductors maintain stability on a ~0.10-s time scale during the burn phase. The dynamic burn model, plasma and engineering energy balances, and stability/equilibrium criteria upon which the RFPR design is based have been described.[2-3] Both technological and economic considerations [3] point to a long-pulsed (0.1-s rise-time, 20-30-s burn period) batch-burn operation using an air-core, superconducting magnet system. Table I summarizes key parameters that define the physics operating point upon which the proposed blanket and power cycle are based.

2. Blanket Design

To the casual observer a magnetically confined fusion reactor appears as an intertwined array of coolant ducts penetrating an almost inaccessible toroidal assembly of superconducting magnets. If the toroidal aspect ratio can be made sufficiently large to allow the use of cyclindrical blanket modules, this problem can be considerably reduced. Furthermore, if the primary confinement system can be combined with the major heating scheme, large auxiliary appendages can be eliminated from the torus, and the system becomes even less complicated. Finally, if the plasma pressure can be supported primarily by poloidal magnetic fields, which characteristically decrease in strength as the minor radius increases, the low-field superconducting coils can be removed from the vicinity of the blanket without a serious increase in stored magnetic energy. The RFP is unique in that it combines all three of these merits: arbitrary aspect ratio, combined heating/confinement system, and low-field poloidal field coils. These physics characteristics [2,3] directly affect favorably the blanket design presented herein. In addition, this design invokes a "conventional" blanket technology embodied in the water/steam cooling of a packed Li_2O bed, stainless-steel structure, and stagnant, borated-water shielding. "Nonconventional" aspects of the RFPR blanket include a copper first wall for plasma stabilization and ambient-temperature feedback coils arrayed between the blanket and shield. Present understanding of the RFP is not sufficient to propose a steady-state reactor, but the long-pulsed reactor [2,3] considerably reduces all system thermal excursions. Batch-burn operation is permitted by the high-beta energy balance, thereby eliminating additional complexities associated with refueling and impurity-control systems.

2.1 Mechanical Layout of Blanket

A schematic view of four RFPR modules (2-m length, 1.5-m-radius first wall) is depicted in Fig. 1. The poloidal field coils (PFC), which provide the plasma heating and primary confinement, are permanently fixed to a structure that is considerably removed from the 12.7-m radius torus and, therefore, are not shown. The low-field (1-2 T), permanently installed, toroidal field coils (TFC) are sufficiently narrow and adequately spaced to permit removal of blanket and shielding modules. Figure 2 illustrates a first-wall/blanket module in more structural detail. The 20-mm-thick copper inner wall operates near the blanket temperature. A mechanical interlock (Fig. 2) between modules provides structural stability and enhanced electrical contact, although an electrically continuous first wall is not necessary for a wall-stabilized plasma. Heat generated in the 0.5-m thick Li_2O blanket (40 v/o Li_2O, 10 v/o H_2O, 15 v/o steel, 35 v/o void) is removed by water/steam circulating in radially oriented U-tubes that are manifolded at the outer blanket radius. These radial coolant tubes are placed on 40-mm centers and support external fins to enhance heat transfer from the Li_2O packed bed. Tritium is removed from the packed bed by a low-pressure helium purge stream. The torus is composed of 40 blanket/shield modules and rests within a vacuum tunnel; each module is provided with a vacuum duct (Fig. 1) that connects the plasma chamber to the vacuum tunnel. Including the copper first wall, a blanket module weighs 60 tonne, which approximately equals the weight of the associated, water-filled (12 w/o H_3PO_3, 18.8 a/o ^{10}B, 1.5-m-thick) shield module. An 80-mm-thick steel and 100-mm-thick-lead region is located between the 0.5-m-thick blanket and the 1.5-m-thick hemi-cylindrical shield to provide gamma-ray attenuation.

2.2 Neutronics Analysis

A one-dimensional, radial transport computation [4] was performed in the P_3S_8 approximation on an 18-zone representation of the first-wall/blanket/shield/coil geometry. For a 14.1-MeV neutron wall loading of 2.5 MW/m^2, the average power density in the blanket is 4.75 MWt/m^2, the tritium breeding ratio is 1.11, and the efficiency for capturing the fusion neutron energy is 99.1%. Table II summarizes the key neutronic results. The local heating rates are used by the thermohydraulic calculations, which, when coupled with the local tritium breeding rate and a tritium diffusion model, yields the spatial and temporal dependence of the tritium release rate and inventory. Although the 20-mm copper first wall represents a net benefit for tritium breeding, the effects the high (n,2n), (n,α) and (n,p) reaction rates (0.1445, 0.0041, 0.0121 per incident neutron, respectively), coupled to the high displacement rate ($\approx 10^{-}$ dpa/s), will present a materials problem and a lifetime determinant for this structure.

2.3 Thermohydraulic Analysis

The thermohydraulic analysis of the first-wall/blanket system is conveniently divided into three parts: the Cu first-wall, the blanket coolant tubes (water/steam), and the Li_2O packed bed. The cooling requirements for the steel/lead (0.0034 MW/m^3) and H_2O/H_3BO_4 ($6.76(10)^{-4}$ MW/m^3) shields are negligible.

2.3.1. First Wall

For the burn conditions given on Table I, the first-wall bremsstrahlung and plasma/field energy fluxes averaged over the burn cycle amount to 0.79 and 0.64 MW/m^2, respectively. The averaged volumetric heating within the copper first-wall and stainless steel backing correspond, respectively, to 33.8 and 9.4 MW/m^3. Because of the batch-burn operation without plasma divertors, the firstwall receives 38% of the total thermal power. A circumferential water-coolant system was selected that is separate from the blanket coolant, although the possibility of using the first-wall region for a preheat or superheat function was considered. The maximum copper temperature was computed by a transient finite-element computer code [5] to be 660 K with a maximum change of 15 K over the burn cycle. Conservatively using 25% of the coolant channel area for heat transport, the maximum heat flux would be 1.32 MW/m^2, compared to 3.1 MW/m^2 estimated [6] for the critical heat flux, neglecting centrifugal body forces. Both temperature gradient and cyclic stress were computed to be below creep and fatigue limits for oxygen-free copper, but the anticipated high rates of transmutation, displacements, and gas generation demands considerably more analysis of the materials problems.

2.3.2 Blanket Coolant Tubes

The coolant U-tubes traverse the Li_2O packed bed radially on 40-mm centers at the first-wall radius; the heat input to all finned U-tubes should be similar. Table III summarizes key thermohydraulic parameters. The fin design was not optimized, but the use of eight external fins of 1.25-m-thickness and 10-mm(4)/4-mm(4) lengths was computed to control satisfactorily the peak Li_2O temperature; this fin arrangement also flattens the radial temperature distribution. The latitude in the fin design variables appears to permit a nearly isothermal blanket, despite the strong variation in nuclear power density. The flow distribution and boiling stability within the two-phase U-tube was carefully quantified. Although the blanket configuration results in all possible tube orientations, the relatively short lengths and low flow velocity should cause flow maldistribution and instabilities that are no worse than found in a conventional steam generator. Furthermore, the low pressure drop makes possible the use of inlet flow orifices to increase the single-phase pressure drop if damping of instabilities proves necessary. [7]

Figure 3 gives the radial distribution of coolant and U-tube temperatures. The transition between single-phase, forced-convection flow was treated by the Jens-Lottes correlation [6] to predict the tube-wall temperature. The transition from subcooled low-quality forced convection to high-quality, forced convection, which occurs at 5-10% quality, was predicted by using the Chen equations [6,7] and is labeled "annular flow" in Fig. 3. The point where the annular liquid layer yields to a higher-quality mist flow or "dryout" was predicted by the Macbeth correlation. [6,7] Beyond the point of dryout the "frozen droplet" model [6,7] was used. In computing the tube wall temperature, a fouling resistance of $1.76(10)^{-6}$ m^2 K/W [6] was used. As seen from Fig. 3, the maximum tube temperature of 781 K occurs in the post-dryout region; use of internal fins to reduce this temperature would allow the exit steam temperature and overall thermal efficiency to be increased. The tube wall temperature was used in conjunction with the local Li_2O power density to compute the packed-bed temperature distribution.

2.3.3 Packed Li_2O Bed

Using the tube temperature distribution, a triangular unit cell (Fig. 3) and the AYER computer program, [5] the Li_2O packed-bed temperature distribution was computed. A triangular unit cell was placed at each radial mesh-point used by the neutronics model. The high-temperature thermal properties of ZrO_2 were used to describe Li_2O, for which only ambient-temperature data could be found. Thermal conductivity correlations for powders [8] were corrected for the presence of atmospheric helium gas (i.e., the tritium purge gas). The radial dependence of the highest Li_2O temperature is also shown in Fig. 3. This "hot spot" temperature occurs at the center of a square formed by four of the triangular unit cells (Fig. 3) and cycles 1.3 K during a RFPR burn.

2.4 Tritium Release

The major concern about tritium revolves about two issues: a) isolation of tritium from the water/steam coolant stream(s), and b) the adequacy of the tritium release rate from the Li_2O particles. The first issue is addressed qualitatively. Low levels (few ppm) of oxygen in the helium purge should rapidly oxidize gaseous tritium, thereby assuring isolation from the U-tube coolant. Isolation of tritium in the plasma chamber from the first-wall coolant also appears feasible, in that diffusion at the 660 K peak temperature would lead to negligible coolant contamination. Hence, given favorable tritium oxidation kinetics in the Li_2O/He packed bed and an integral copper first wall, tritium contamination in either coolant loop should not present a serious problem. This question, however, must be examined in more detail, particularly with respect to the first-wall coolant loop.

The second tritium issue focuses on the rate of fuel supply and blanket inventory required for a self-sufficient system. The unit cell used to compute the Li_2O radial "<u>macro</u>distribution" of temperature (Fig. 3) was applied to the kinetics of tritium build-up and release. Each radial position is occupied by Li_2O particles of nominal radius r_p. The local Li_2O pellet temperature and power density allows an estimate of the "<u>micro</u>distribution" of temperature throughout the pellet. If the pellet of radius r_p is assumed to be composed of individual grains of radius, r_g, the time-dependent diffusion equation could be applied to that grain at a temperature given by the microdistribution. The tritium partial pressure at each grain boundary was assumed equal to that surrounding the Li_2O pellet (i.e., rapid grain boundary difusion), and the tritium diffusivity for a given grain was evaluated according to the microdistribution of temperature within the pellet. Tritium release and inventory at any time is summed over all grains in a pellet; this summing procedure is continued over all pellets situated along the macrodistribution of temperature, as given by the thermohydraulic calculations (Fig. 3). Following this numerical procedure allows the time and space evolution of the tritium concentration and release to be determined within a given unit cell at a given radial position as a function of assumed diffusion coefficient, grain radius, r_g, and pellet radius, r_p. Finally, these tritium distributions are integrated over the entire blanket to yield the total tritium inventory I(kg/m), release rate L(kg/s m), and production rate R(kg/s m). Figure 4 shows the dependence of I/Rt and L/R on time t for a range of realistic r_p and r_g values. For the tritium diffusivity assumed (i.e., for BeO [9]), the Li_2O macrodistribution of temperature given in Fig. 3 indicated only ~ 80% equilibrium (tritium production equals release) after a number of years. The results presented in Fig. 4 corresponds to a macrodistribution of temperature in which the thermal unit cell closest to the first wall was repeated radially outward through the blanket. Generally, the system will become self-sufficient in tritium when the value of L/R exceeds the inverse of the tritium breeding ratio. Packed beds with the largest pellet radius (enhanced temperature peaking within a pellet) and smallest grain size (enhanced diffusive loss) give a breakeven time of $7(10)^5$ s, that increases to $1(10)^8$ s for the smaller pellets and larger grain sizes. None of these cases achieve an equilibrium blanket inventory within a projected lifetime, but after five years the tritium retained in the blanket typically lies in the range 0.3–1.0 kg/m (8.2–27.3 kg/GWt). The value of tritium diffusivity used for Li_2O, as well as radiation effects on both tritium transport and changing pellet morphology, represent important uncertainries.

3. Power Cycle

Steam from the blanket is used to drive directly a high-pressure turbine operating with a Rankine, direct cycle; the blanket would operate both as a steam generator and a superheater. The wet-steam cycle is similar to that used for light-water fission reactors (Table IV). The first-wall coolant loop removes 38% of the total thermal energy, but this loop must operate with lower coolant temperatures (Table III). The water (460 K) leaving the first-wall coolant loop is used first for reheat between the intermediate and low-pressure turbines (460/445 K), and a liquid-liquid heat exchanger (445/427 K) is used to heat feedwater returning to the packed-bed blanket. Finally, a low-temperature (427/310 K) isobutane boiler is used for a bottoming cycle before returning the first-wall cooling water.

The gross efficiency of this low-superheat cycle is 26.5%. Moderate changes in the blanket design are required to adopt a boiling water or pressurized-water fission reactor cycle, which operates above 30% efficiency. The constraints presently envisaged for the copper first wall, however, will not allow a complete adoption of either fission reactor conditions and efficiencies. Parametric studies show that operating the first wall at the blanket coolant temperature would increase the cycle efficiency to 29%. Increasing the blanket/first-wall coolant temperatures by 100 K above those reported in Table IV would result in cycle efficiencies of 35%. Operating with higher coolant temperatures, however, will require a reassessment of the conventional materials used.

4. Conclusions

A steam-generating packed-bed blanket using conventional materials and fabrication technologies appears feasible from the viewpoint of tritium containment, operations and maintenance, thermalhydraulics, structural adequacy, and overall steam cycle. Although cycle efficiencies of 30% are generally possible with this conventional approach, the presently perceived need for a 20-mm-thick conducting first wall for the RFPR reduces this efficiency to 26.5%. Since this copper first wall intercepts 38% of the total thermal energy, operation of the conducting first wall near ambient temperature would lead to considerably reduced cycle efficiencies. The first-wall configuration adopted for this study plays an important role in the achievement of acceptable tritium breeding ratios in relatively thin structure-filled blankets, but the radiation effects, as measured by transmutation, gas production, and displacement rates, will be significant. Although the conducting first wall is not a structural member or a vacuum barrier, the potential for increased electrical resistivity and loss of self-integrity may require frequent replacement and/or repair. It is emphasized, however, that present physics understanding is sufficiently obscure to warrant examination of other schemes and configurations to provide short-term (<0.1-s) plasma stabilization while simultaneously maintaining an acceptable breeding ratio and cycle efficiency. Lastly, the use of two separate coolant loops and a low-temperature bottoming cycle is not the most cost-effective approach, and, consequently, future studies and refinements of this blanket concept will focus on an integrated first-wall/blanket coolant system in which the first-wall region will function as a preheater.

REFERENCES

[1] KRAKOWSKI, R. A., HAGENSON, R. L., MILLER, R. L., MOSES, R. W., "Systems Studies and Conceptual Reactor Designs of Alternative Fusion Concepts at LASL," Proc. 7th Conf. on Plasma Physics and Controlled Nuclear Fusion Research, Innsbruck, Austria (August 23-30, 1978).

[2] HAGENSON, R. L., KRAKOWSKI, R. A., "An Engineering Design of a Toroidal Reversed-Field Re ctor (RFPR)," Proc. 10th Symp. on Fusion Technology, Padova, Italy (September 4-8, 1978).

[3] HAGENSON, R. L., KRAKOWSKI, R. A., "A Cost-Constrained Design Point for the Reversed-Field Pinch Reactor (RFPR)," Proc. 3rd ANS Topical Meeting on the Technology of Controlled Nuclear Fusion, Santa Fe, New Mexico (May 9-11, 1978).

[4] HILL, T. R., "ONETRAN: A Discrete Ordinate, Finite Element Code for the Solution of a One-Dimensional Multigroup Transport Equation," Los Alamos Scientific Laboratory report LA-5996-MS (June 1975).

[5] LAWTON, R. G., "The AYER Heat Conduction Computer Program," Los Alamos Scientific Laboratory report LA-5613-MS (May 1974).

[6] ROHSENOW, W. H., "Boiling," Handbook of Heat Transfer, ROHSENOW, W. H., HARTNETT, J. P. (eds), Sec. 13, pp. 13.34-13.63, McGraw-Hill Book Company, NY (1973).

[7] LAHEY, R. J., JR., MOODY, F. J., The Thermal-Hydraulics of a Boiling Water Nuclear Reactor, p. 331, Amer. Nucl. Soc. Monograph Series (1977).

[8] GODBEE, H. W., ZIEGLER, W. T., "Thermal Conductivities of MgO, Al_2O_3, and ZrO_2 Powders to 850°C; I, Experimental," J. Appl. Phys. 37, 1, 40-55 (January 1966).

[9] ELLEMAN, T.S., ZUMWALT, L. R., VERGHESE, K., "Hydrogen Transport and Solubility in Non-Metallic Solids;" Proc. 3rd ANS Topical Meeting on the Technology of Controlled Nuclear Fusion, Santa Fe, New Mexico (May 9-11, 1978).

TABLE I. RFPR-II INTERIM DESIGN SUMMARY: AIR-CORE POLOIDAL TRANSFORMER, SUPERCONDUCTING COILS

Parameter	Value
First-wall radius (m)	1.5
Major radius (m)	12.8
Plasma current (MA)	20.0
Toroidal coil energy (GJ)	4.7
Poloidal coil energy (GJ)	6.6
Burn time (s)	21.6
Cycle time (s)	26.6
14.1-MeV neutron current (MW/m^2)	2.5
Engineering Q-value	6.5
Thermal power (MWt)	2950
Power density[(a)] (MWt/m^3)	0.90

(a) Based on volume enclosed by and including superconducting coils.

TABLE II. NEUTRONIC PARAMETERS (I_W = 2.5 MW/m^2) EXPRESSED PER UNIT LENGTH OF PLASMA

Parameter	Value
Total tritium breeding ratio	1.112
^{6}Li breeding ratio	0.970
^{7}Li breeding ratio	0.142
Heating in the blanket (MW/m)	
neutron	15.7
gamma	10.4
Total	26.1
Heating in the shield (MW/m)	
neutron	0.03
gamma	0.21
Total	0.24
Total heating in the coil (W/m)	0.91
Helium[(a)]/hydrogen[(a)]/dpa[(b)] production	
first wall (Cu)[(c)] × 10^{-3}	4.08/12.10/
structure (steel near first wall) × 10^{-3}	0.46/1.55/
structure (steel near outer blanket) × 10^{-3}	0.03/0.12/
coil (Cu) × 10^{-13}	6.46/28.40/

(a) per incident neutron

(b) per second

(c) (n,2n) = 0.1445 per incident neutron

TABLE III. THERMAL HYDRAULIC PARAMETER FOR A 2-m LONG BLANKET MODULE

Parameter	First Wall	Blanket U-Tube
Material	Cu	Fe/Cr/Ni
Radial thickness (m)	0.02	0.5
Water flow rate (kg/s)	39.6	19.7
Inlet pressure (MPa)	5.52	5.5(nominal)
Pressure drop (kPa)	21	< 1.4
Inlet temperature (K)	310	310
Outlet temperature (K)	460	551
Number of coolant passages	100	5890
Dimensions of coolant channel (mm)	15 × 15	12.5 o.d. (1.0 wall)
Flow rate per channel (kg/s)	0.4	$3.4(10)^{-3}$
Reynolds number	$7.6(10)^4$	$4.74(10)^6$[(a)]
Maximum temperature (K)	660	781
Minimum temperature (K)	549	475
Flow velocity (m/s)	1.63	0.04 (inlet)

(a) 22,000 at steam outlet

TABLE IV. SUMMARY OF STEAM CYCLE CONDITIONS

Parameter	RFPR	BWR/6[(a)]	PWR[(b)]
Rated Output (MWt/MWe)	2950/790	3293/1000	2568/886
System pressure (MPa)	5.5	6.9	15.1 (primary) 6.3 (secondary)
Steam generator temperatures (K)			
inlet	422	558	508
outlet	551	--	572
Superheat (K)	7.8	0.0	19.4
Total coolant flow rate (kg/s)	1584(first wall) 768 (blanket)	1777	8273 (primary) 702 (secondary)
Total heat transfer area (m^2)	764 (first wall)[(c)] 12,000 (blanket)	— —	4620 (core) 28,000 (steam generators)
Steam generator tubes			
number	$2.76(10)^5$	—	31,960
length (m)	1	--	18
temperature (K)	844	--	589
pressure, (MPa)	6.2	—	7.2
Overall thermal-to-electric conversion efficiency	0.265	> 0.3	> 0.3

(a) boiling-water fission reactor

(b) pressurized-water fission reactor

(c) based on 25% of total cooling duct area

FIGURE CAPTIONS

Fig. 1. Isometric view of 2-m-long RFPR reactor modules(4). Entire assembly is located within a vacuum trench that is lined vertically with the poloidal field coils (not shown).

Fig. 2. Isometric view of 2-m-long RFPR blanket module illustrating replacement scheme.

Fig. 3. Temperature and power distributions in the Li_2O packed bed, coolant tube and coolant.

Fig. 4. Time dependence of normalized tritium blanket inventory I(kg/m) and release rate R(kg/s m) for a Li_2O(40 v/o) packed bed of 0.5-m thickness as a function of Li_2O pellet radius r_p and grain radius r_g, using BeO tritium diffusivity.[9] Case 10 indicates pellet conditions where local melting of Li_2O is expected.

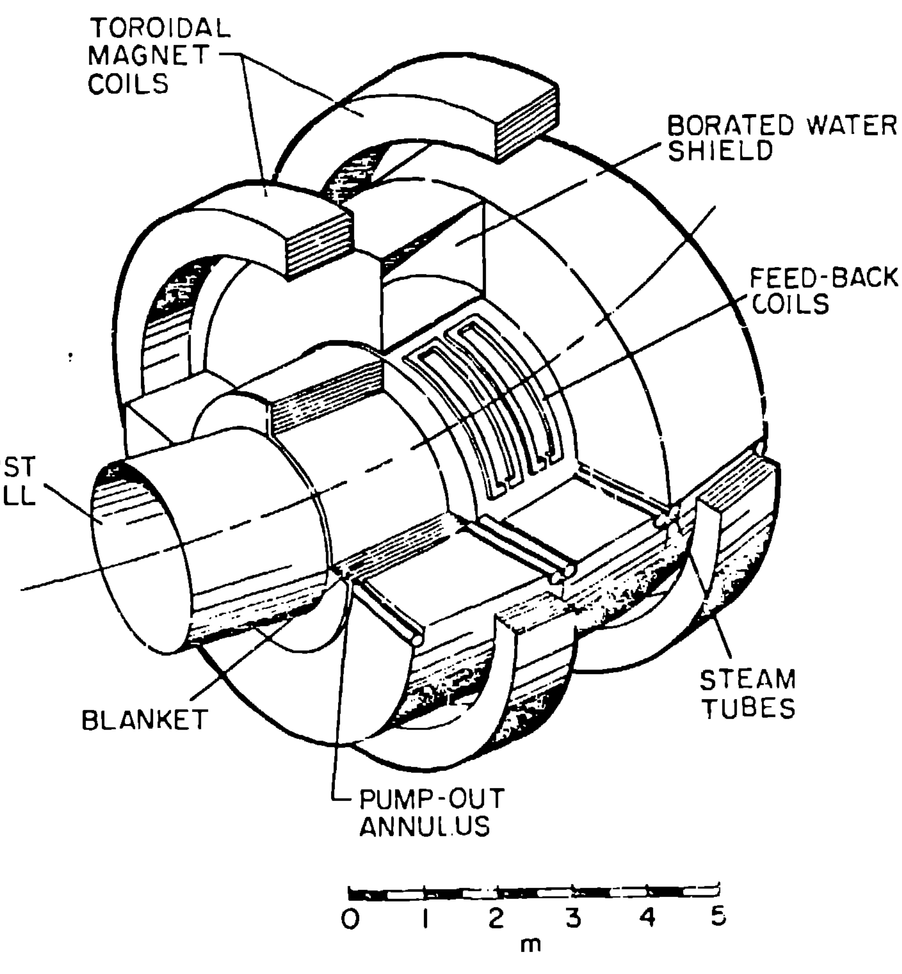
TOROIDAL
MAGNET
COILS
BORATED WATER
SHIELD
FEED-BACK
COILS
FIRST
WALL
BLANKET
STEAM
TUBES
PUMP-OUT
ANNULUS
0 1 2 3 4 5
m

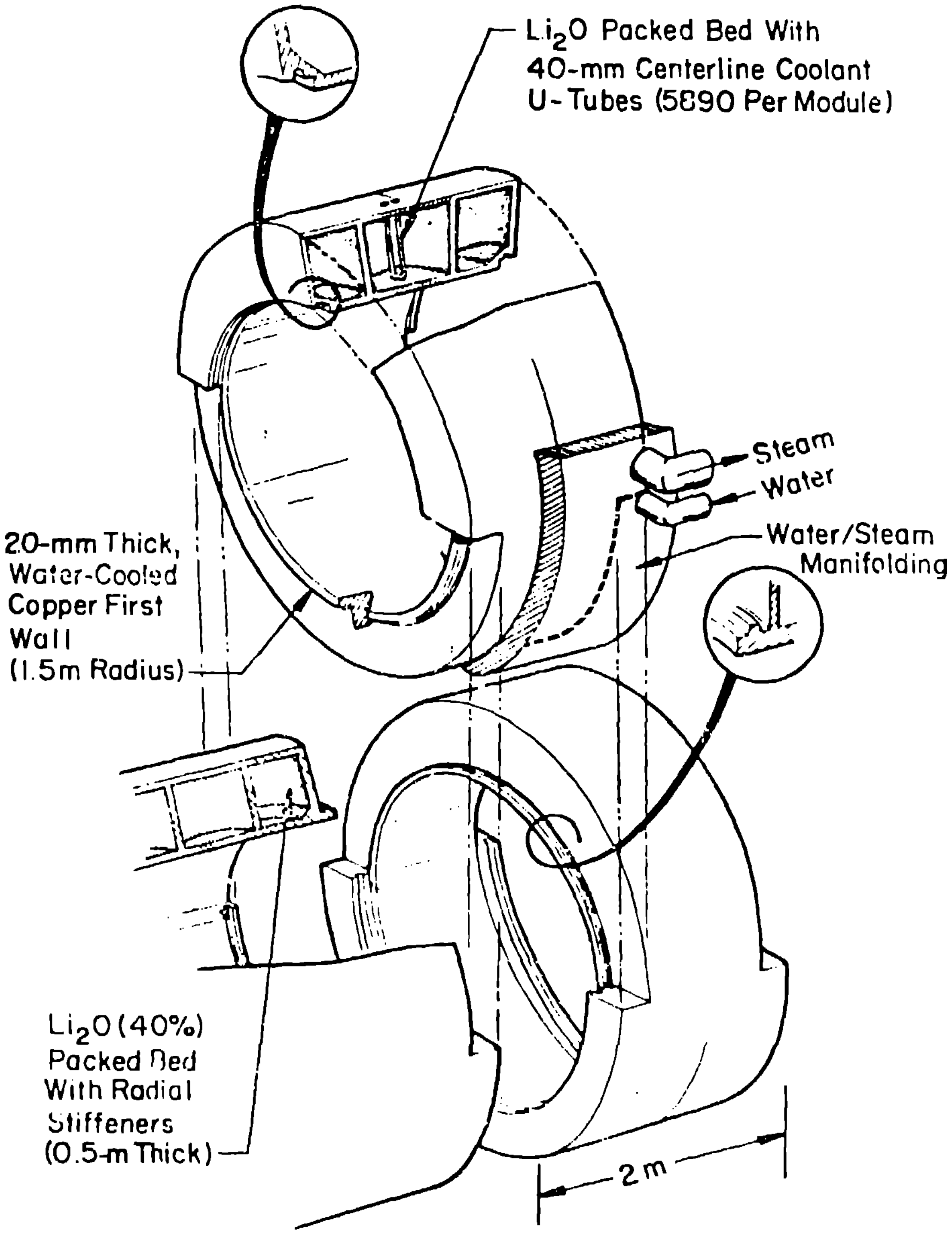

Li_2O Packed Bed With
40-mm Centerline Coolant
U-Tubes (5890 Per Module)
Steam
Water
Water/Steam
Manifolding
20-mm Thick,
Water-Cooled
Copper First
Wall
(1.5m Radius)
Li_2O (40%)
Packed Bed
With Radial
Stiffeners
(0.5-m Thick)
2 m

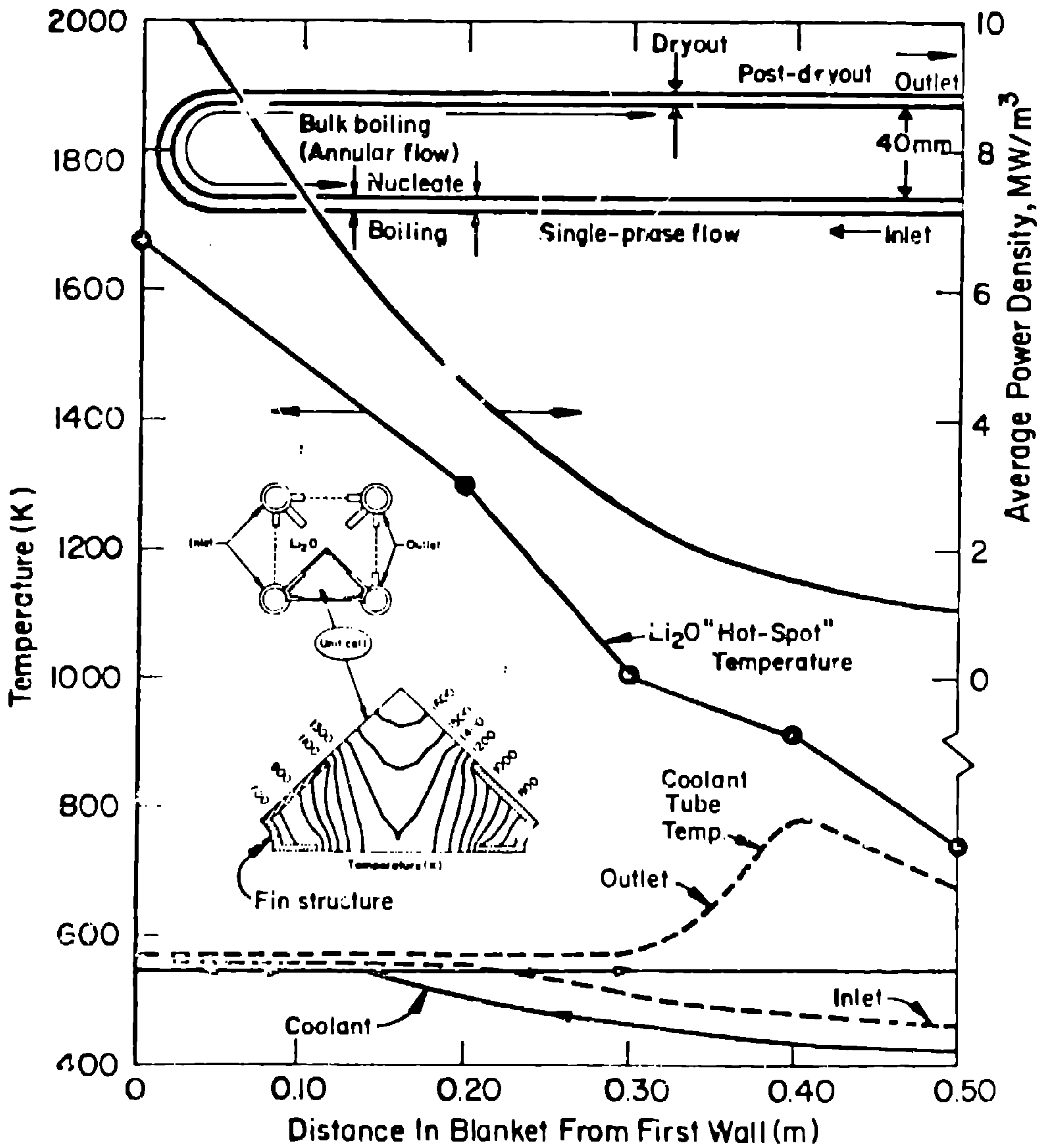

2000
1800
1600
1400
1200
1000
800
600
400
10
8
6
4
2
0
0
0.10
0.20
0.30
0.40
0.50
Temperature (K)
Average Power Density, MW/m³
Distance In Blanket From First Wall (m)
Dryout
Post-dryout
Outlet
Bulk boiling
(Annular flow)
40mm
Nucleate
Boiling
Single-phase flow
Inlet
Li2O "Hot-Spot"
Temperature
Coolant
Tube
Temp.
Outlet
Inlet
Coolant
Fin structure

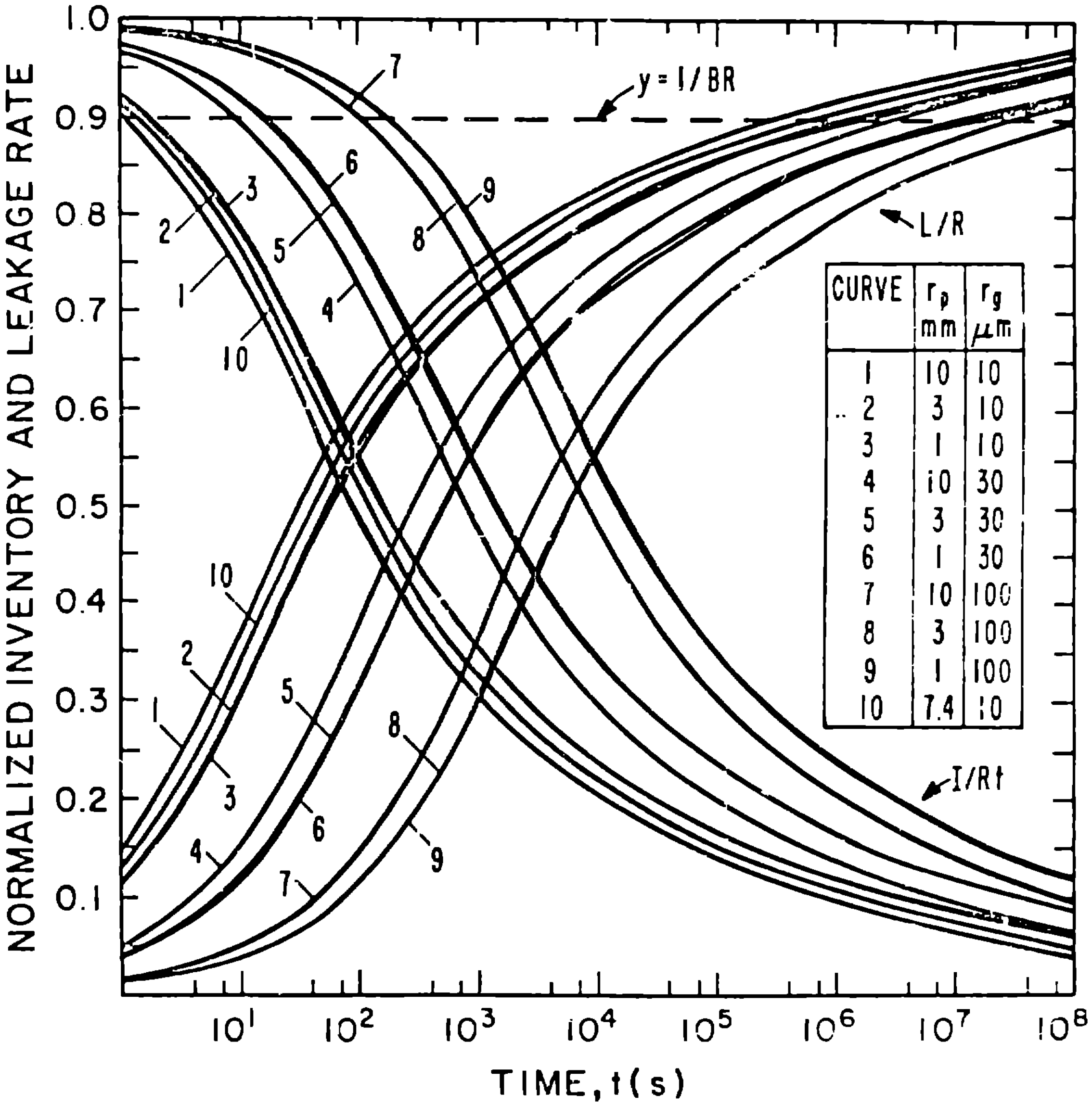
NORMALIZED INVENTORY AND LEAKAGE RATE
TIME, t (s)
y = 1/BR
L/R
I/Rt
CURVE | r_p mm | r_g μm
1 | 10 | 10
2 | 3 | 10
3 | 1 | 10
4 | 10 | 30
5 | 3 | 30
6 | 1 | 30
7 | 10 | 100
8 | 3 | 100
9 | 1 | 100
10 | 7.4 | 10